Progress In Electromagnetics Research, Vol. 116, 171–184, 2011

PREDICTION OF THE ELECTROMAGNETIC FIELD IN METALLIC ENCLOSURES USING ARTIFICIAL NEURAL NETWORKS

M. Luo and K. Huang

School of Electronics and Information Engineering
Sichuan University, Chengdu 610064, China

Abstract—In complex electromagnetic (EM) environment, EM field distribution inside a metallic enclosure is determined by the external EM radiation and emissions from internal contents. In the design of an electronic system, we usually need to estimate the EM field level in a concerned region inside the enclosure under various EM environments. In this paper, we use artificial neural network (ANN), rather than full wave analysis, combined with the numbered measurements to predict the EM field in the concerned region inside a metallic enclosure. To verify this method, a rectangular metallic enclosure with a printed circuit board (PCB) is illuminated by external incident wave. The measured electric fields inside the enclosure combined with ANN model based on back propagation (BP) training algorithm are used to estimate the values of electric field. The calculation is fast and predictions reveal good agreement with the measurements that validate this method.

1. INTRODUCTION

Due to complex EM environment, metallic enclosures are widely used to protect most of the electronic and electrical systems from unintentional and/or intentional EM interference. However, in most practical applications, slots, holes, and even apertures have to be created on the walls of the enclosure for signal wiring, power supply, and heat dispersion. Unfortunately, these structures create EM energy coupling paths that allow external EM field to propagate into the enclosure, thus they degrade the shielding effectiveness [1–6]. In addition, the internal circuits which can produce EM radiation will

Received 11 March 2011, Accepted 28 April 2011, Scheduled 4 May 2011
Corresponding author: Ming Luo (mingheroluo@tom.com).

increase the EM complexity significantly in the metallic enclosure. Their radiation and different locations will change the EM field distribution in the enclosure, and then the induced signal may exceed the given threshold values and thus produce nonlinear behaviors, malfunctions or irreversible damages in an integrate circuits or other components. So, in the optimization of system design, we need to evaluate whether an important vulnerable and high-sensitivity IC or semiconductor component could be disturbed in various EM environments.

In order to handle these problems, some methods have been proposed in the past year. Numerical method such as 3-D full wave analysis method based on the Maxwell's equations including the Finite Difference Time Domain (FDTD) [7–11], Finite Element Method (FEM) [12–14] and Moment Method (MoM) [15–17], has been used for analyzing these problems. Some hybrid numerical techniques [18–20] and transmission-line method [21–24] are also developed to analyze the enclosure. However, the numerical method is severely limited by the size of the enclosure. To achieve reasonable accuracy, one must choose a grid size small enough to resolve the apertures, but the enormous number of cells requires a large computer memory and computation time. Along with these numerical approaches, analytical and semi-analytical methods [25–27], are also used to analyze the shielding effectiveness of metallic enclosures, they are fast and efficient but are only applicable for very simple geometries and approximate treatment. In an actual system design, we usually estimate the EM field in advance under various locations of internal circuits and external incident fields, but the field in the enclosure varies with different locations of internal circuits and external incident field, and it is impossible to solve all different states by solving one or several calculations.

These constraints motivate us to apply artificial neural network (ANN) method to handle this problem. In this paper, we use ANN model based on back propagation (BP) training algorithm, rather than full wave analysis, combined with numbered measurements to predict the EM field in a metallic enclosure. In our ANN models, the nodes in the input layer represent the parameters of location of the PCB, field strength of external incident wave, the polarization angle and incident angle, etc, which influence the inner field of enclosure. There exist some nodes in the hidden layer for nonlinear mapping. The nodes in the output layer represent the prediction field. To validate this method, a rectangular metallic enclosure with an aperture and a printed circuit board (PCB) illuminated by an external incident wave has been studied. Numerical examples show that the results predicted by the trained ANN are in good agreement with those results obtained

by measurement. Neural networks are very powerful, with the use of ANN, the fast and preliminary prediction for the inner field under different EM conditions can be made.

2. GEOMETRY OF THE SYSTEM

Consider the rectangular metallic enclosure with dimensions of $a \times b \times c = 50 \times 100 \times 100$ cm and manufactured by six aluminum sheets of thickness 5 mm as shown in Fig. 1(a) to verify the proposed method. There is an aperture with dimensions of $t \times s = 12.5 \times 11$ cm in its front wall. A PCB as shown in Fig. 1(b) is placed into the enclosure from the center of the upper wall via a mechanical instrument. The PCB is composed of a limiter, microstrip patches. The patches performing like an antenna working at the central frequency of 2.5 GHz. It can produce an intentional EM radiation to imitate the interference effect of radiation from internal electronic circuits. Moreover, it can be rotated horizontally to represent different circuit locations. The limiter is an active component with VSWR $\leq$ 1.3 at 2–3 GHz and predetermined threshold level of 10 dBm. The load is used to match the PCB and absorb the excess energy. The incident plane wave is provided by the far field of a broadband ridged horn antenna. A rectangular horn antenna is used to receive external incident field and the received power is transmitted to the circuit via a coaxial cable. A monopole antenna is used to measure the field for training sample sets and the ANN model is trained by the measured data. The system is set up inside an anechoic chamber. The photograph of the actual structure of the system is shown in Fig. 2.

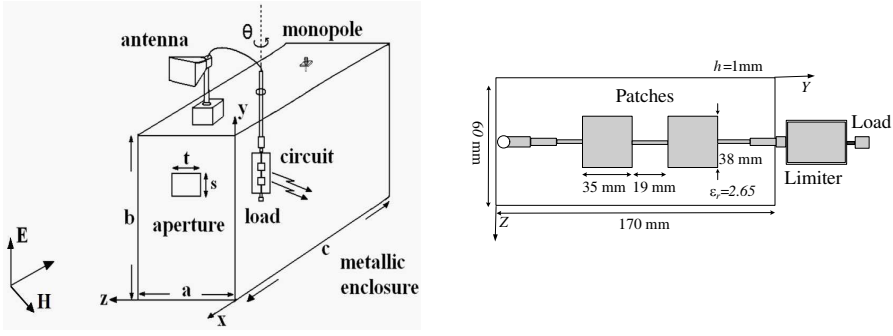

Figure 1. Structures of rectangular metallic enclosure with a PCB (a) Enclosure illuminated by external incident wave, (b) The PCB.

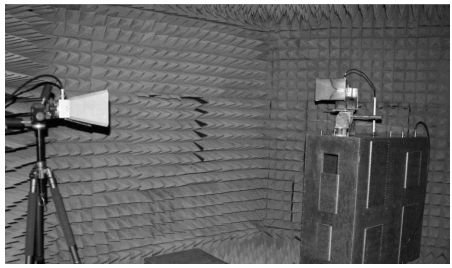

Figure 2. Photograph of the actual fabricated metallic enclosure in anechoic chamber.

3. MODEL BASED ON ANN TECHNIQUE

Here, we use ANN model based on BP training algorithm, rather than full wave analysis, to predict the EM field in the enclosure. Fast, accurate and reliable neural network models can be developed from measured or simulated microwave data. Once developed, these neural models can be used in place of computational EM models to speed up microwave investigation [28–30].

3.1. ANN Technique Introduction

In an ANN model, a neuron is an information-processing unit that is fundamental to the operation of a neural network. The block diagram of Fig. 3(a) shows the model of a neuron, which forms the basis for designing ANN. In mathematical terms, we may describe a neuron by writing the following equation:

$$o_k = f\left(\sum_{j=1}^{m} w_{kj} i_j + b_k\right) \tag{1}$$

where k is the neuron number, i_1, i_2, ..., i_m are the input parameters; w_{k1}, w_{k2}, ..., w_{kj} are the weights of neuron; b_k is the bias; O_k is the output parameter; f is the effect of applying an affine transformation to the output.

Typically, a network as shown in Fig. 3(b) consists of a set of sensory units that constitute the input layer, one or more hidden layers, and an output layer [31, 32]. The neuron number l, m and n in each layer are respected to input parameters, hidden neuron number and output parameters, respectively. The nodes in the input layer represent the effective parameters on inner field. The nodes in the hidden layer are used to nonlinear mapping, an appropriate value for

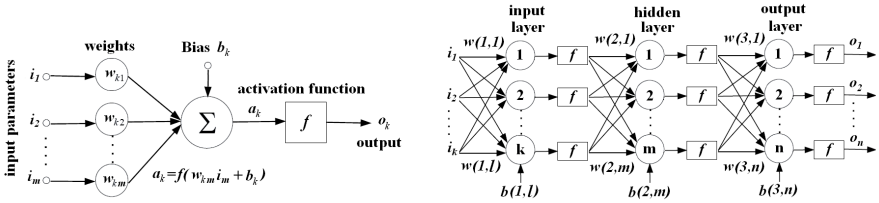

Figure 3. The ANN model based on BP training algorithm. (a) Model of a neuron, (b) neural network framework for prediction.

m can avoid the overlearning and underlearning problems [33], their choice is usually based on the experience and early research data, it can be calculated by the approximate expression ($m = \mathrm{sqrt}(l+n)+q$, q is integer from 1 to 10). The nodes in the output layer represent the results of prediction. Supervised learning arithmetic which using the steepest gradient descent method to reach any small approximations is adopted. The training process is described by the following equations to update these weights, bias values. The output of the jth neuron in the hidden layer is calculated by following steps:

$$net_j = \sum_{i=1}^{k} w_{2,i} i_i + b_{2,j} \quad j = 1, 2, \ldots, m. \tag{2}$$

$$a_j = f_{hidden}(net_j) \qquad j = 1, 2, \ldots, m. \tag{3}$$

where net_j is the activation value, a_j is the output of the hidden layer, and f_{hidden} is called the activation function which is usually a linear, sigmoid or tansig function. The sigmoid used in this model is described as:

$$f_{hidden}(x) = \frac{1}{1+\exp(-x)} \tag{4}$$

The outputs of the p neuron in the output layer are given as bellow:

$$o_p = f_{output}\left(\sum_{i=1}^{m} w_{3,i} i_i + b_{3,i}\right) \quad p = 1, 2, \ldots, n. \tag{5}$$

where f_{output} is the activation function, usually a linear function. All weights are assigned with random values initially, and are modified by the delta rule according to the learning samples traditionally. Mean squared error (MSE) is selected as the search objective of our approach which is written as:

$$MSE = \sum_{i=1}^{n} (\alpha - \tau)^2 \tag{6}$$

where α presents the authentic values which are already known, such as simulated or measured data, τ is the output values of the trained neural network. Our goal is to minimize the MSE making sure that the prediction is closer to the true as possible as they can.

3.2. ANN Based Prediction Modeling Technique

A drawing of a metallic enclosure with a circuit is shown in Fig. 1. The field in the enclosure is produced by the coupling of external incident wave from aperture and the internal radiation of circuit. To estimate the EM field in enclosure under various placements of internal circuits and external incident field, a three-layer BP neural network as shown in Fig. 4 is used to solve the EM interference problem. The interference parameters, such as incident direction, polarization characteristic, incident electric intensity, placement of circuit and frequency, construct the input layer of the ANN model. Several nodes in the hidden layer are used to nonlinear mapping. The output layer represents the predicted voltage which then can be described by using ANN as follows:

$$V_o = F_{ANN}\left(E^i, \Lambda, \varphi, \gamma, \theta, f\right) \tag{7}$$

where F_{ANN} represents ANN model of each Interference parameters. It can be found that the predicted voltage (V_o) is a function of $E^i, \Lambda, \varphi, \gamma, \theta$ which represent the incident electric intensity, incident direction (Λ, φ), polarization characteristic, placement of circuit and frequency, respectively.

Once the inputs and outputs are identified, training data needs to be generated. In this paper, the training data sets are obtained directly from numbered measurement and the number of samples is chosen that the ANN model accurately represents the original problem. A uniform sampling strategy is selected that each input parameter is sampled at equal intervals. The order of magnitude of input parameter values in this application can be very different for the input parameters

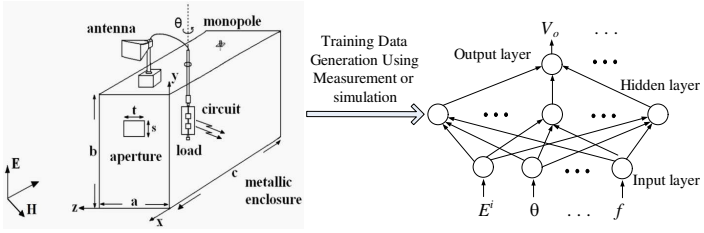

Figure 4. The ANN model for the EM interference problem.

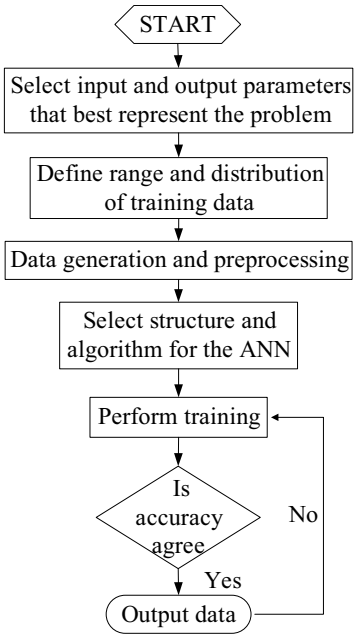

Figure 5. The whole steps involved in neural model development.

have different physical dimension, a data scaling technique is used to improve the training process which is given by [33]

$$\bar{x} = x_{\min} + \frac{x - x_{\min}}{x_{\max} - x_{\min}}(x_{\max} - x_{\min}) \tag{8}$$

where $\bar{x}$ and x represent a generic element in the vectors of scaled and not scaled data, respectively, ($x_{\min}$, $x_{\max}$) is the range of input parameter.

The training was conducted by using BP algorithm until the difference between the training data and the output from the ANN model has reached less than 0.1%. The whole steps involved in ANN model development is shown in Fig. 5 After the ANN model has been trained, it can use to predict in different conditions.

4. EXAMPLES AND DISCUSSION

In this section, numerical examples are given to show the process of using the ANN method described above to solve the EM interference problem. Assume the location of the monopole antenna is the concerned region where an important, vulnerable and high-sensitivity

device will be stored. Firstly, we should get the training sample set by measuring the internal electric field. Then, we use the obtained data to train the ANN model and finally predict the results by the trained model.

4.1. Measure the EM Field

A monopole antenna as shown in Fig. 1(a) is used to sense the field in the enclosure. Its output connector is connected to port of spectrum analyzer terminated in a 50-Ω load. In this way, the output power P_o of the monopole antenna is accurately measured by the spectrum analyzer. Then, the output monopole antenna voltage V is calculated as follows:

$$V = \sqrt{P_o Z_o} \tag{9}$$

where $Z_o = 50\,\Omega$ is the characteristic impedance of type N connector. When P_o is measured, we can get voltage V from (9) easily and evaluate the electric field level in the enclosure.

4.2. Neural Network Training and Test

As a first example, we research the influence of circuit location in the enclosure. We rotate the PCB as shown in Fig. 1 to imitate various locations of internal circuit and predict the electric field under arbitrary rotation angle θ of the PCB through numbered measurements. In order to construct such a model, the number of nodes in the input layer of the ANN is set to be $l = 1$ which represents the rotation angle θ of the PCB. It is the interference parameter for electric field strength. The number of nodes in the hidden layer is set to be $m = 11$ which is used for nonlinear mapping. The number of nodes in the output layer is set to be $n = 1$ which represents the predicted induced voltages.

In the learning phase, we use numbered measurements to train the ANN model. The rotating platform above the enclosure can rotate from 0 to 180 degree. The electric field strength in different rotation angle θ of the PCB is measured in this range for the training sample points. The sampling interval is $\Delta\theta = 10^\circ$, so there are 19 training sample points are used to train the model. In the predicting phase, other 6 test points which are selected in the range of $[0^\circ, 180^\circ]$ and different from the training points are used to validate the prediction. Ranges and sampling levels for the training and test points are given in Table 1.

The microwave power source produces an incident plane wave at 2.5 GHz and offers a constant power level in the process. The system is illuminated by the external incident wave. Fig. 5 shows the electric

Table 1. The training and test points for the model.

Input parameters	Notation	Values in sampled levels	Sampling interval
Training samples	θ	$(0^\circ \sim 180^\circ)$ 19-level sampling	$\Delta\theta = 10^\circ$
Test samples	θ	$(0^\circ \sim 180^\circ)$ 6-level sampling	$\Delta\theta = 30^\circ$

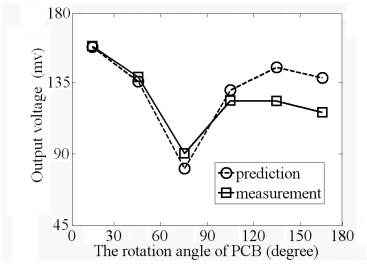

Figure 6. The comparison of prediction and measurements.

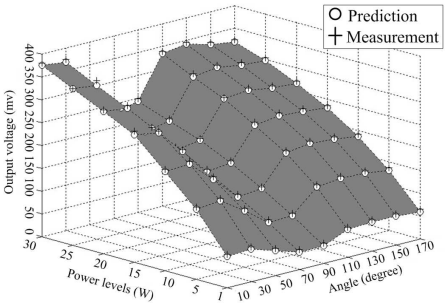

Figure 7. The comparison of measured and predicted results at 2.5 GHz under different rotation angles and radiation power levels (a) $\theta = 30^\circ$; (b) $\theta = 90^\circ$; (c) $\theta = 150^\circ$.

field strength for different rotation angle θ of PCB predicted by the neural network model. For comparison, the measurements are also given in Fig. 6. It shows that they are in agreement.

The field in the enclosure is determined by both the radiation coupled from aperture and radiation of the PCB. The presence of the circuit which has active component makes the field complicated. Therefore, it is clearly that the internal electric field strength will not proportional to the external radiation power level. In the next example, external incident field, as an interference parameter, is also included in the ANN model. We will predict the electric field strength in the enclosure under different rotation angle θ of the PCB and external incident field through numbered measurements.

The neural network for this model is the same as the previous model except that the number of input nodes is set to be $l = 2$ which represent interference parameters of rotation angle θ of PCB and external radiation power levels. The number of nodes in the hidden

layer and output layer are set to be $m = 12$ and $n = 1$, respectively. The rotation angle θ of PCB and the external radiation power level P_r for the training sample sets are selected in the range of $[0°, 180°]$ with sampling interval of $\Delta\theta = 10°$ and $[1W, 30W]$ with sampling interval of $\Delta p = 5W$, respectively. Thus there are 133 training sample points are used to train the model. The electric field strength for test sample points which are different from the training points is also measured. Ranges and sampling levels of the input parameters θ and P_r for the training and test points are given in Table 2. The microwave power source produces an incident plane wave at 2.5 GHz to illuminate the system. The power levels are set by adjusting the transmitted power of the antenna.

After training the ANN model, we used it to predict. For the test points, arbitrary values in the given ranges as described in Table 2 are selected to validate the predictions. The comparison of the prediction and measurement results at 2.5 GHz under different rotation angles and radiation power levels are given in Fig. 7. The prediction error is shown in Fig. 8, the maximal error is less than 9%. The results show

Table 2. Training and test points for the model.

Input parameters		Notation	Values in sampled levels
Training samples	Rotation	θ	$(0° \sim 180°)$ 10-level sampling
	Radiation power	P_r	$(1W \sim 30W)$ 7-level sampling
Test samples	Rotation	θ	Arbitrary values in the range of $0° \sim 180°$
	Radiation power	P_r	Arbitrary values in the range of $1W \sim 30W$

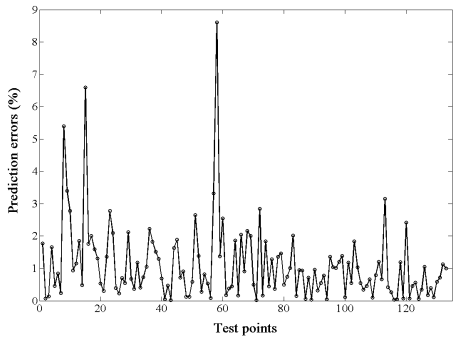

Figure 8. Prediction errors of prediction data sets and test data sets.

that they are in good agreement, and validate that the trained ANN model can predict the electric field strength at an arbitrary rotation angle θ of PCB and radiation power level in the given ranges.

All of the numerical computations above were executed on our computer with a CPU of AMD Core 2 1.91 GHz and 4 GB RAM. All the input and output parameters are normalized into values in the range of $[0, 1]$ by data scaling technology during the computation [33]. The time required in the training work of one neural network model is not more than 10 minutes. However, the numerical methods such as FDTD will generate a large number of grid cells and require several hours or more time for the field in the same enclosure. Although the time consumed in the measurement and training increases with the size of ANN model, it can be completed in advance. The main advantage of using ANN method is that it's almost real-time in prediction. In addition, the prediction is accurate from the engineering point of view.

5. CONCLUSION

In this paper, the ANN method is introduced to predict the EM field in the metallic enclosure. The influence parameters for field in the enclosure are extracted to construct the ANN model. Although, only location of PCB and external radiation power level are included in the paper, it could be used to construct for a more complex system. The expression of method described here simply serves as a catalyst. It doesn't need 3D model and long time of computation, but only needs some training data which obtained by measurement or simulation. Once the ANN model for the problem is trained, it can predict the EM field and give a quick answer in various internal and external EM environments. Although the training of an ANN model is usually time consuming, it can be completed in advance. Numerical examples show that the results predicted by the ANN models are consistent with those obtained by measurements and this method can be used in the application of the enclosure analysis.

ACKNOWLEDGMENT

This project is supported by the National Science Foundation of China under Grant No. 60871064.

REFERENCES

1. Xie, H., J. Wang, R. Fan, and Y. Liu, "Spice models for radiated and conducted susceptibility analyses of multiconductor shielded

cables," *Progress In Electromagnetics Research*, Vol. 103, 241–257, 2010.

2. Faghihi, F. and H. Heydari, "Reduction of leakage magnetic field in electromagnetic systems based on active shielding concept verified by eigenvalue analysis," *Progress In Electromagnetics Research*, Vol. 96, 217–236, 2009.
3. Bahadorzadeh, M. and M. N. Moghaddasi, "Improving the shielding effectiveness of a rectangular metallic enclosure with aperture by using extra shielding wall," *Progress In Electromagnetics Research Letters*, Vol. 1, 45–50, 2008.
4. Ghafoorzadeh, A. and K. Forooraghi, "Analysis of an inclined semi-circular slot in the narrow wall of a rectangular waveguide," *Progress In Electromagnetics Research*, Vol. 90, 323–339, 2009.
5. Ahmed, S. and Q. A. Naqvi, "Directive EM radiation of a line source in the presence of a coated PEMC circular cylinder," *Progress In Electromagnetics Research*, Vol. 92, 91–102, 2009.
6. D'Amore, M. and M. S. Sarto, "Theoretical and experimental characterization of the EMP-interaction with composite-metallic enclosures," *IEEE Trans. Electromagn. Compat.*, Vol. 42, 152–163, May 2000.
7. Cerri, G., R. de Leo, and V. M. Primiani, "Theoretical and experimental evaluation of the electromagnetic radiation from apertures in shielded enclosures," *IEEE Trans. Electromagn. Compat.*, Vol. 34, 423–432, Nov. 1992.
8. Lei, J. Z., C. H. Liang, and Y. Zhang, "Study on shielding effectiveness of metallic cavities with apertures by combining parallel FDTD method with windowing technique," *Progress In Electromagnetics Research*, Vol. 74, 82–112, 2007.
9. Swillam, M. A., R. H. Gohary, M. H. Bakr, and X. Li, "Efficient approach for sensitivity analysis of lossy and leaky structures using FDTD," *Progress In Electromagnetics Research*, Vol. 94, 197–212, 2009.
10. Li, M., J. Noebel, J. L. Drewniak, R. E. DuBroff, T. H. Hubing, and T. P. van Doren, "EMI from cavity modes of shielding enclosures-FDTD modeling and measurements," *IEEE Trans. Electromagn. Compat.*, Vol. 42, 29–38, Feb. 2000.
11. Xu, K., Z. Fan, D.-Z. Ding, and R.-S. Chen, "Gpu accelerated unconditionally stable crank-nicolson FDTD method for the analysis of three-dimensional microwave circuits," *Progress In Electromagnetics Research*, Vol. 102, 381–395, 2010.
12. Carpes, Jr., W. P., L. Pichon, and A. Razek, "Analysis of

the coupling of an incident wave with a wire inside a cavity using an FEM in frequency and time domains," *IEEE Trans. Electromagnetic Compatibility*, Vol. 44, No. 3, 470–475, Aug. 2002.

13. Carpes Jr., W. P., L. Pichon, and A. Razek, "A 3D FEM model for EMC analysis: Coupling of an EM wave with a wire inside a cavity," *Proc. Int. Symp. Elecromagnetic Fields in Electrical Engineering (ISEF'99)*, 57–60, Pavia, Italy, Sep. 1999.
14. Benhassine, S., L. Pinchon, and W. Tabbara, "An efficient finite-element time-domain method for the analysis of the coupling between wave and shielded enclosure," *IEEE Trans. Magn.*, Vol. 38, No. 2, 709–712, Mar. 2002.
15. Ebadi, S. and K. Forooraghi, "Green's function derivation of an annular waveguide for application in method of moment analysis of annular waveguide slot antennas," *Progress In Electromagnetics Research*, Vol. 89, 101–119, 2009.
16. Rajamani, V., C. F. Bunting, M. D. Deshpande, and Z. A. Khan, "Validation of modal/MoM in shielding effectiveness studies of rectangular enclosures with apertures," *IEEE Trans. Electromagn. Compat.*, Vol. 48, No. 2, 348–353, May 2006.
17. Klinkenbusch, L., "On the shielding effectiveness of enclosures," *IEEE Trans. Electromagn. Compat.*, Vol. 47, No. 3, 589–601, Aug. 2005.
18. Chiariello, A. G., G. Miano, and A. Maffucci, "An hybrid model for the evaluation of the full-wave far-field radiated emission from PCB traces," *Progress In Electromagnetics Research*, Vol. 101, 125–138, 2010.
19. Sarto, M. S., "Hybrid MFIE/FDTD analysis of the shielding effectiveness of a composite enclosure excited by a transient plane wave," *IEEE Trans. Magn.*, Vol. 36, No. 4, 946–950, Jul. 2000.
20. Tharf, M. S. and G. I. Costache, "A hybrid finite element-analytical solutions for inhomogeneously filled shielding enclosures," *IEEE Trans. Electromagn. Compat.*, Vol. 36, No. 4, 380–385, Nov. 1994.
21. Duffy, P., T. M. Benson, and C. Christopoulos, "Application of Transmission Line Modeling (TLM) to studying the effectiveness of screened enclosures," *IEE Colloq. Screening of Connectors, Cables Enclosures*, 2/1–2/3, Jan. 17, 1992.
22. Kraft, H., "Modeling leakage through finite apertures with TLM," *Proc. IEEE Int. Symp. Electromagnetic Compatibility*, 73–76, Aug. 22–26, 1994.
23. Argus, P., P. Fischer, A. Konrad, and A. J. Schwab, "Efficient

modeling of apertures in thin conducting screens by the TLM method," *Proc. IEEE Int. Symp. Electromagnetic Compatibility*, 101–106, Vol. 1, Aug. 21–25, 2000.

24. Attari, R. and K. Barkeshli, "Application of the transmission line matrix method to the calculation of the shielding effectiveness for metallic enclosures," *Proc. IEEE Antennas Propagation Soc. Int. Symp.*, 302–305, Vol. 3, Jun. 16–21, 2002.
25. Méndez, H. A., "Shielding theory of enclosures with apertures," *IEEE Trans. Electromagn. Compat.*, Vol. 20, 296–305, May 1978.
26. Robinson, M. P., T. M. Benson, C. Christopoulos, J. F. Dawson, M. D. Ganley, A. C. Marvin, S. J. Porter, and D. W. P. Thomas, "Analytical formulation for the shielding effectiveness of enclosures with apertures," *IEEE Trans. Electromagn. Compat.*, Vol. 40, 240–248, Aug. 1998.
27. Wallyn, W., F. Olyslager, E. Laermans, D. de Zutter, R. de Smedt, and N. Lietaert, "Fast evaluation of the shielding efficiency of rectangular shielding enclosures," *Proc. IEEE Int. Symp. Electromagnetic Compatibility*, 311–316, Seattle, WA, Aug. 1999.
28. Christodoulous, C. and M. Georgiopoulos, *Applications of Neural Networks in Electromagnetics*, Artech House, Boston, MA, 2001.
29. Zhang, Q. J. and K. C. Gupta, *Neural Networks for RF and Microwave Design*, Artech House, Norwood, MA, 2000.
30. Hasar, U. C., G. Akkaya, M. Aktan, C. Gozu, and A. C. Aydin, "Water-to-cement ratio prediction using anns from nondestructive and contactless microwave measurements," *Progress In Electromagnetics Research*, Vol. 94, 311–325, 2009.
31. Haykin, S., *Neural Networks: A Comprehensive Foundation*, Prentice Hall, Upper Saddle River, NJ, 1994.
32. Rumelhart, D. E., G. E. Hinton, and R. J. Williams, *Parallel Distributed Processing*, Vol. I, 318–362, D. E. Rumelhart and J. L. McClelland (eds.), MIT Press, Cambridge, MA, 1986.
33. Devabhaktuni, V. K., M. Yagoub, Y. Fang, J. Xu, and Q. J. Zhang, "Neural networks for microwave modeling: Model development issues and nonlinear modeling techniques," *Int. J. RF Microwave Computer-aided Eng.*, Vol. 11, 4–21, 2001.